行政院國家科學委員會專題研究計畫　成果報告

氫原子磁振造影及頻譜儀對股骨頭缺血性骨壞死的評估及預測（2/2）

計畫類別：個別型計畫
計畫編號：NSC90-2314-B-002-412-
執行期間：90 年 08 月 01 日至 92 年 01 月 31 日
執行單位：國立臺灣大學醫學院放射線科

計畫主持人：施庭芳

計畫參與人員：台大醫學院　侯勝茂教授

報告類型：精簡報告

處理方式：本計畫可公開查詢

中　華　民　國 92 年 6 月 27 日

Proton MR Spectroscopy of the Femoral Head - Evaluation of Patients at Risk for Avascular Necrosis

Tiffany Ting-Fang Shih, M.D.
Department of Radiology
National Taiwan University, Medical College and Hospital
No.7, Chung-Shan S Rd. Taipei, Taiwan

文 章 尚 未 發 表 ， 內 容 請 勿 公 開

Abstract:

To measure the lipid / water ratio of the femoral head from normal individuals and also, the non-diseased femoral head from patients with contralateral avascular necrosis (AVN) using proton magnetic resonance spectroscopy (MRS). Twenty-four femoral heads from 12 normal subjects and 15 non-diseased femoral heads from patients with contralateral AVN were included. Marrow composition was measured by using single-voxel stimulated-echo acquisition method (STEAM) (TR/TE = 5000/20 msec) with a voxel placed in the femoral head. The area under each resonance for lipid and water was calculated.

The area of lipid (L) to area of water (W) ratio (L/W ratio) of the femoral head was significantly different between the patients with AVN on the contralateral side and normal individuals (P = 0.0048), this ratio revealing a greater value for those at risk of AVN. This detected difference appears to precede any other morphological change associated with AVN, such an increase in L/W ratio possibly suggesting the pathogenic route for AVN.

Key words: Magnetic Resonance (MR)

Proton MR Spectroscopy (MRS)

Lipid and Water

Avascular Necrosis (AVN)

Femoral Head (FH)

Bone Marrow

Introduction:

Avascular necrosis (AVN) of the femoral head is an important and largely unresolved problem in orthopedic surgery. The pathomechanism is considered to arise due to impairment of femoral head blood perfusion and/or increased intraosseous pressure (IOP). Hungerford and Zizic, in 1983, proposed a developmental mechanism for the condition based upon an intraosseous, extravascular derangement that subsequently results in a perfusion abnormality (1). As the bone presents as a Starling resister, it can be seen that any increase in the pressure within intraosseous extravascular compartment would result in a decrease in bone medullary blood flow, the fundamental concept being that cancellous bone functions as a closed compartment (2). Within this closed space, small, thin-walled, collapsible vessels provide the blood supply and drain the marrow spaces (2). An elevation in IOP will then be transmitted to small collapsible vessels within the bone, thus causing a decrease in blood flow to the bone and bone marrow. Rapid or uncompensated increases in IOP are thought to result in irreversible ischemic, and subsequent tissue damage. Tissue damage causes edema, which further elevates pressures within the closed marrow compartment.

The internal environment of the femoral head is composed of fatty bone marrow (80% fat), water, trabecular bone and myeloid cells. The vascularity in the fatty

marrow is less substantial than in the case for the red marrow (3). Thus, any metabolic anomaly of the fat component will readily result in increased IOP. As is suggested in the literature, corticosteroid treatment is an important etiologic factor that leads to the occurrence of avascular necrosis (4), such treatment eliciting derangement in fat metabolism and leading to an increase in the fat deposition in peripheral tissue such as the marrow spaces of bone (5, 6). Further, lipocyte hypertrophy may result from corticosteroid treatment (7). Within the closed space of the femoral head, lipocyte hypertrophy is thought to impede perfusion of the marrow (7, 8). Thus, alteration of intramedullary fat cell metabolism will lead to a bone marrow perfusion change within the femoral head, ultimately resulting in avascular necrosis (9).

Magnetic resonance (MR) imaging has been demonstrated to disclose marrow changes resulting from the AVN of the femoral head (10-15). Such MR signal patterns for AVN have been described as varying widely. Exampling this, Bassett et al presented, in 1987, the preoperative MR image of a resected ischemic necrotic femoral head and neck, and disclosed a subchondral focus of diminished signal intensity of a transudate of proteinaceous material with probable calcifications, the adjacent region of normal, high signal intensity representing "mummified" fat (10). These authors also revealed that the next lower stratum of diminished signal intensity was composed of fibrous and vascular tissues and histiocytic infiltrates. In that same

year, Mitchell et al (12) demonstrated the "double line sign" peripheral to the necrotic femoral head, the group also describing a central region within the rim which was isointense for marrow fat on both T1- and T2-weighted images. Lang et al (1988) also revealed high signal-intensity necrotic marrow mixed with low signal intensity (14).

The above data suggest that the (MR) signal patterns deriving from the necrotic area of the femoral head largely reflect the signal changes corresponding to fat cell necrosis, since fat cells constitute the dominant portion of the femoral head. On the other hand, the signal pattern from viable or dead fat cell contained within the bone, strongly reflect the MR signals deriving from an example of AVN of the femoral head. Thus, further investigation of the fat content of the femoral head was considered as necessary, particularly by using different parameters, such as MR spectroscopy (MRS), in addition to MR images.

In 1995, Bluemke et al tried to measure the fat content (as a percentage) in the femoral head by using MRS upon patients with systemic lupus erythematosus who displayed no evidence of avascular necrosis, as well testing long-term corticosteroid treatment patients and healthy subjects (16). Ballon et al (1991) used the volume-localized MRS technique to estimate the bone marrow cellularity and found the result was well correlated with the results from marrow-core biopsies (17). Shick et al used double spin-echo sequences in 1992 to measure the spectra in the vertebral

bodies (18). This group compared the water signal distributions from healthy people and patients after bone marrow transplantation and revealed a relative difference between the two. A year later, the same group also demonstrated the fat-water ratio and qualities of water and lipid protons from leukemic red marrow using MRS (19). Following chemotherapy, evidence suggests that lipid and water content normalize for successfully-treated leukemic patients (19). In 1997, Amano et al used the stimulated echo pulse sequence technique to demonstrate a significant difference in marrow water to fat ratio between patients with aplastic anemia and healthy subjects (20). Schellinger et al (1999) used a similar technique to measure the lipid-water ratio and line width of 82 normal subjects, the results of which appeared to be correlated with gender and age (21).

The above-mentioned MRS technique is mainly applicable to the red, hematopoeitic marrow of the vertebral body (17-21), only Bluemke et al applying it to the yellow, fatty marrow of the femoral head in a 1995 study (16). The alteration of the fat to water ratio of the yellow marrow may result in a change to the blood perfusion in the femoral head, which was important to the subclinical or early stages of non-traumatic AVN. The MRS technique is considered by our group to be one of the most convenient methods to perform as an *in vivo* study of the femoral head with associated provision for follow up study. Thus, we performed the MRS technique to

study the (asymptomatic) hips of patients who had exhibited non-traumatic AVN in the contralateral hip, in addition to the hips of normal subjects, with the expectation that we would be able to detect alterations of lipid to water ratio of the femoral head prior to the presentation of any morphological evidence of AVN.

Materials and Methods:

Normal individuals and patients with unilateral AVN of the femoral head were included in this study. All patients and normal subjects who participated provided informed consent disclosures prior to their participation.

Twelve normal individuals (nine male, and three female) were recruited to participate in this study. The average age of the normal subjects was 47 years (range, 20 - 67 years). None of the patients revealed any history of corticosteroid use, or any other known risk factors for avascular necrosis or any history of hip pain, although from the group,. six men and two women had previous experience with chronic lower back pain.

Fifteen patients (eleven male, and four female) were recruited for this study. The average age of the patients was 43 years (range, 23 - 70 years). All participating patients exhibited unilateral AVN of the femoral head ranging from stage II to stage IV (Table 1). The contralateral femoral head for all of these participating patients revealed no evidence of AVN as determined by plain radiography and MR examinations and, in addition, the contralateral joint remained asymptomatic.

The osteonecrotic femoral heads were treated by vascularized bone grafts (n = 9), total hip replacement (n = 1) and conservative methods (n = 5). Four patients revealed a history of hyperbaric scuba diving for at least five years, two revealed a history of

alcohol drinking, and three patients revealed a history of corticosteroid use. All the normal individuals and patients had been subjected to MR imaging and (H-1) MRS analysis in the period. For two of the normal individuals, we elected to repeat the MRS of the femoral head in order to confirm the technique's reproducibility. All MR studies were performed with a 1.5-T whole body MR imaging system (Vision Plus, Siemens Magnetom, Erlangen, Germany). Firstly, in order to assess for the condition of the femoral head, the imaging protocol commenced with a T1-weighted SE sequence (TR/TE 500/12 msec) of coronal planes of 4mm thickness and with a 0.8 mm slice gap. The second component of this analysis incorporated a turbo sequence of short tau inversion recovery (STIR) (TR/TE/Ti 4300/30/170 msec, turbo factor = 7) of coronal planes of same thickness and gap. Another turbo SE T2-weighted sequence (TR/TE 6,000/90 msec, turbo factor = 11) was conducted in a transaxial planes of the same dimension and spatial relationship as above. The (H-1) MRS technique incorporated the use of a single-voxel stimulated-echo acquisition method (STEAM), and was performed by using a $1.25 \times 1.25 \times 1.25$cm (cubic) voxel held in location by three-dimensional localization: central portion of the femoral head. The other operational parameters are TR/TE 5000/20 msec (21). The use of TR at a level of 5,000ms allows for observing fully T1-relaxed magnetic resonance, and maintaining TE set at 20ms minimizes MR signal reduction due to the T2 effect. For the normal

individuals, femoral head MRS was performed bilaterally. For the patients with unilateral AVN, MRS was performed only on the non-diseased, asymptomatic femoral head. The areas under the water and lipid spectra and the peak amplitude of the lipid were determined by using the associated Siemens spectroscopy computer processing software.

Result:

The MR imaging results were interpreted first, any patient data revealing either an abnormal signal or evidence of AVN of the femoral head being rejected. There was no apparent evidence suggesting avascular necrosis, bone marrow edema or degenerative arthritis for bilateral femoral heads of the normal individuals and the non-diseased femoral head from any of the patients. For the diseased femoral head group from the participating patients, avascular necrosis was identified as being present at a number of different stages, both with or without metallic artifacts resulting from previous surgical procedure, being noted.

Spectroscopic Analysis

The bone marrow signal from the thirty-nine femoral heads examined with MRS measurement all exhibited a high intensity for subcutaneous fat on the T1-weighted images, and a low intensity for fat on turbo STIR images for both hips from the normal individuals (n = 24) and the non-diseased hips from AVN patients (n = 15). All MRS exhibited one water and one dominant lipid peak, separated by 3.1ppm (or 210 Hz). The lipid spectrum exhibited a similar, steep line shape. The water spectrum varied. The areas under the water and lipid curves were defined as pointing 20 continuous points for each with Siemens spectroscopy computer processing software.

The lipid and water spectra were partially overlapping. The differentiation between lipid and water spectra was made at the lowest point of the component of the curves reflecting the overlapping section. The base line of the spectrum was defined as emanating from the lowest point of the curve and extending horizontally. The value of area and peak amplitude was calculated. As presented in Table 2, the areas under lipid and water spectra for the non-diseased femoral heads for 15 patients with AVN on the contralateral side are summarized. The area of lipid (L) revealed a mean value and a standard deviation. The area of water (W) demonstrated a mean value and a standard deviation. The ratio of lipid area to water area (L/W ratio) exhibited a mean value and a standard deviation of. For the 24 hips corresponding to the 12 normal individuals, the data listed in Table 3 reveal the following, an area of lipid (L) with a mean value and a standard deviation. The area of water (W) presents a mean value of and a standard deviation, and the L/W ratio presents a mean value and a standard deviation. For the L/W ratio, the difference between the patients group (n = 15) and the normal individuals group (n = 24) was substantially different (P = 0.0048).

The peak amplitude under the lipid spectrum for the 15 non-diseased femoral heads of the AVN patients revealed a mean value with a standard deviation, and for the 24 femoral heads of the 12 normal individuals, the mean value was with a standard deviation, no difference being demonstrated between these two groups (P =

0.3771).

Discussion:

Magnetic resonance imaging is the most sensitive and well established method for the diagnosis of AVN of the femoral head (10-14). The signal changes and MR pattern for AVN of femoral heads reflected principally as the fat signal from the necrotic bone marrow. The contrast material-enhanced or dynamic contrast-enhanced MR images proved to be able to reliably detect the perfusion changes in the femoral head at least as early as conventional MR images, or possibly even earlier, as observed in the other studies (22-26). According to the known pathophysiology of AVN (7, 9), the alteration of fat composition might be the earliest finding of the femoral head at risk for avascular necrosis.

The most sensitive in vivo determination of bone marrow fat is possible with MRS. Several investigators (eg 17-20, 27, 28) have used the MRS technique to evaluate the lipid and water spectra of bone marrow at lumbar vertebra for the patients with leukemia, aplastic anemia and Gaucher's disease. Only Bluemke et al (1995) used MRS to measure the fat content of the yellow marrow of the femoral head, their study using as the single-voxel stimulated-echo acquisition method with TR 2,000/TE 20, 40, 60 and 80 (16). In these authors' study, the percentage fat content in the femoral head was similar for both the healthy subjects group and for the group of patients with systemic lupus erythematosus who were determined to be at risk for

avascular necrosis. In 1999, Schellinger et al used the method with the parameter TR5,000/TE 20 to evaluate the status of lumbar vertebra for normal subjects and confirmed that the lipid-water ratio progressed with age in a linear fashion for both genders (21). In our study, the use of TR 5,000 msec allows for observing fully T1-relaxed magnetic resonance. Keeping TE at 20 msec minimizes the MR signal reduction due to the T2 effect. All spectra exhibited a water peak to the left and a dominant, steep lipid peak to the right on the respective spectral images, separated by 3.1 ppm. The water spectrum varied. By using this long TR and short TE parameters, we have successfully demonstrated the lipid and water spectra of the yellow, fatty marrow of the femoral head.

Typically, AVN of the femoral head is bilateral. As has been reported previously, the asymptomatic hip of patients who already suffer from AVN in the contralateral hip expresses a likelihood of also succumbing to AVN of between 50 and 72 percent (29-31). Our patients with the femoral heads at risk for AVN (as listed in Table 1) exhibit substantially different values for the lipid to water ratio as measured by *in vivo* proton MRS as compared to normal subjects, suggesting that the alteration of the lipid to water ratio of the femoral head occurred prior to the development of any obvious morphological changes. The lipid to water ratio of the femoral heads at risk for AVN reveal a greater mean value than that corresponding to normal individuals. It showed

statistically significant difference between these two groups (P = 0.0048).

There are several pathogenetic routes leading to avascular necrosis. A change in the intraosseous compartment would result in an increased intraosseous pressure and a decrease in medullary bone blood flow (1). One of the important developmental mechanisms of AVN is the fat-cell changes which take place in the femoral head, as is typically noted to occur for cortisone-treated animals (7, 9). Under histological examination, the marrow fat cells increased by more than ten micrometers in diameter and the epiphyseal fat-cell volume fraction exhibited an increase of 25 to 28 percent following steroid treatment (7). The increased fat-cell size certainly must compress the only compressible space in the femoral head, ie the sinusoidal vascular bed, resulting in a variety of ischemic changes (9). The measurement of fat-cell area is based upon volume estimations deriving from the two-dimensional, planar histological specimens, whereas for the fat spectrum measured by MRS, the data were acquired from a three-dimensional voxel within the bone marrow. The mean lipid to water ratio (L/W) of the femoral head was elevated for those at an elevated risk of AVN as compared with those normal individuals. This finding was considered to have more etiologic significance because the relative lipid fraction (L/[L+W]) could reflect the change of tissue composition within a closed chamber such as the femoral head. The noted increase in the lipid fraction must be accommodated by a reduction of

either the hematopoietic cells, trabecular bone or the vascular sinusoidal component of the marrow space. Clearly thus, compression of the most compressible structures in the space, the sinusoids, must soon follow.

In conclusion, the lipid and water spectra of the femoral head measured by proton MRS proved to be useful for evaluating the progressive development of avascular necrosis. An increase of the mean lipid to water ratio of the femoral heads at risk for avascular necrosis compared to controls is noted to be detectable prior to any morphological changes that may be observed to occur, and might suggest a potential pathogenic factor. In the future, we propose to conduct a subsequent serial follow-up utilizing MRS of the femoral heads of subjects at risk for avascular necrosis.

Reference:

1. Hungerford DS, Zizic TM. Pathogenesis of Ischemic Necrosis of Femoral Head. Hip 1983; 249-262.
2. Wiekes CH, Visscher MB. Some Physiological Aspects of Bone Marrow Pressure. J Bone and Joint Surg (am) 1975; 57:49-57.
3. Vogler JB, Murphy WA. Bone Marrow Imaging. Rad 1988; 168: 679-693.
4. Zizic TM, Marcoux C, Hungerford DS, Dansereau JV, Stevens MB. Corticosteroid therapy associated with ischemic necrosis of bone in systemic lupus erythematosus. Am J Med 1985; F79: 596-604.
5. Solomon L. Mechanisms of Idiopathic Osteonecrosis. Orthop Clin North Am 1985; 16: 655-667.
6. Solomon L. Idiopathic Necrosis of the Femoral Head: Pathogenesis and Treatment. Can J Surg 1981; 4: 270-275.
7. Wang GJ, Sweet DE, Reger SI, Thompson RC. Fat-cell Changes as a Mechanism of Avascular Necrosis of the Femoral Head in Cortisone Treated Rabbits. J Bone and Joint Surg (am) 1977; 59: 729-735.
8. Wang GJ, Lennox DW, Reger SI, Stamp RC. Cortisone Induced Intra-Femoral Head Pressure Changes and its Response to a Drilling Decompression Method. Clin Orthop 1981; 159: 274-278.
9. Hou SM, Liu TK, Kao MC. Studies on Corticosteroid-Induced Avascular Necrosis of Femoral Heads in Rabbits. J Biomedical Science 1994; 1: 61-64.
10. Bassett LW, Mirra JM, III AC, Gold RH. Ischemic Necrosis of the Femoral Head. Clinical Orthopaedics and Related Research 1987; 223: 181-187.
11. Mitchell DG, Joseph PM, Fallon M, Hickey W, Kressel HY, Rao VM, Steinberg

ME, Dalinka MK. Chemical-Shift MR Imaging of the Femoral Head: An In Vitro Study of Normal Hips and Hips with Avascular Necrosis. AJR 1987; 148: 1159-1164.

12. Mitchell DG, Rao VM, Dalinka MK, Spritzer CE, Alavi A, Steinberg ME, Fallon M, Kressel HY. Femoral Head Avascular Necrosis: Correlation of MR Imaging, Radiographic Staging, Radionuclide Imaging, and Clinical Finding. Radiology 1987; 162: 709-715.
13. Markisz JA, Knowles RJR, Altchek DW, Schneider R, Whalen JP, Cahill PT. Segmental Patterns of Avascular Necrosis of the Femoral Heads: Early Detection with MR Imaging. Radiology 1987; 162: 717-720.
14. Lang P, Jergesen HE, Moseley ME, Block JE, Chafetz NI, Genant HK. Avascular Necrosis of the Femoral Head: GHigh-Field Strength MR Imaging with Histologic Correlater. Radiology 1988; 169: 517-524.
15. Beltran J, Herman LJ, Burk JM, et al. Femoral Head Avascular Necrosis: MR Imaging with Clinical-Pathologic and Radionucleide Correlation. Radiology 1988; 166: 215-220.
16. Bluemke DA, Petri M, Zerhouni EA. Femoral Head Perfusion and Composition: MR Imaging and Spectroscopic Evaluation of Patients with Systemic Lupus Erythematosus and at Risk for Avascular Necrosis. Radiology 1995; 197: 433-438.
17. Ballon D, Jakubowski A, Gabrilove J, Graham MC, Zakowski M, Sheridan C, Koutcher JA. In Vivo Measurements of Bone Marrow Cellularity Using Volume-Localized Proton NMR Spectroscopy. Magnetic Resonance in Medicine 1991; 19: 85-95.
18. Schick F, Bongers H, Jung WI, Skalej M, Lutz O, Claussen CD.

Volume-Selective Proton MRS in Vertebral Bodies. Magnetic Resonance In Medicine 1992; 26: 207-217.

19. Schick F, Einsele H, Bongers H, Jung WI, Skalej M, Duda S, Ehninger G, Lutz O. Leukemic Red Bone Marrow Changes Assessed by Magnetic Resonance Imaging and Localized H Spectroscopy. Hematol 1993; 66: 3-13.

20. Amano Y, Kumazaki T. Proton MR Imaging and Spectroscopy Evaluation of Aplastic Anemia: Three Bone Marrow Patterns. Journal of Computer Assisted Tomography 1997; 21(2): 286-292.

21. Schellinger D, Lin CS, Fertikh D, Hatipoglu H, Davis BT. Lumbar proton MRS: Lipid-water ratio and line width in normal subjects-Diagnostic potentials Radiology 1999;213(p),357..

22. Vande Berg BC, Malghem J, Labaisse MA, Noel H, Maldague B. Avascular Necrosis of the Hip: Comparison Of Contrast-Enhanced and Nonenhanced MR Imaging with Histologic Correlation Work in Progress. Radiology 1992; 182: 445-450.

23. Nadel SN, Debatin JF, Richardson WJ, Hedlund LW, Senft C, Rizk WS, Malizos KN, Stahl DL, Martinez S. Detection of Acute Avascular Necrosis of the Femoral Head in Dogs: Dynamic Contrast-Enhanced MR Imaging vs. Spin-Echo and STIR Sequences. AJR 1992; 159: 1255-1261.

24. Cova M, Kang YS, Tsukamoto H, et al. Bone Marrow Perfusion Evaluated with Gadolinium-Enhanced Dynamic Fast MR Imaging in a Dog Model. Radiology 1991; 179: 535-539.

25. Tsukamoto H, Kang YS, Jones LC, et al. Evaluation of Marrow Perfusion in the femoral Head by Dynamic Magnetic Resonance Imaging: Effect of Venous Occlusion in a Dog Model. Invest Radiol 1992; 27: 275-281.

26. Langer R, Langer M, Scholz A, Astinet F, Schwetlick G, Felix R. Femoral Head Perfusion in Patients with Femoral Neck Fracture and Femoral Head Necrosis. J Belg Radiol 1993; 76: 145-149.

27. Shick F, Einsele H, Lutz O, Claussen CD. Lipid Selective MR Imaging and Localized H Spectroscopy of Bone Marrow During Therapy of Leukemia. Anticancer Research 1996; 16: 1545-1552.

28. Jensen KE, Jensen M, Grundtvig P, Thomasen C, Karle H, Henriksen O. Localized in Vivo Spectroscopy of the Bone Marrow in Patients with Leukemia. Magn Reson Imaging 1990; 8: 779-789.

29. Boettcher WG, Bonfiglio M, Hamilton HH, Sheets RF, Smith K. Non-Traumatic Necrosis of the Femoral Head. Part 1: Relation of Altered Hemostasis to Etiology. J. Bone and Joint Surg (am) 1970; 52A: 312-321.

30. Steinberg ME, Hayken GD, Steinberg DR. The conservative Management of Avascular Necrosis of the Femoral Head. Bone Circulation, edited by Arlet J, Ficat RP and Hungerford DS, Williams and Wilkins, Baltimore, 1984, P334-337.

31. Jergesen HE, Shabi Khan A. The Natural History of Untreated Asymptomatic Hips in Patients Who Have Non-Traumatic Osteonecrosis. J Bone and Joint Surg (am) 1997; 79A: 359-363.

Table 1. Clinical Data from Patients with Unilateral Avascular Necrosis of the Femoral Head.

Case No.	Age/Sex	*AVN Side & Stage	**Duration (months)	Therapeutic method	Etiologic Associations
1	47 M	R, III	39	vascularized bone graft	Diving hyperbaric
2	48 M	L, III	36	vascularized bone graft	Diving hyperbaric

3	44 M	R, II	2	vascularized bone graft	Nil
4	50 M	R, II	35	vascularized bone graft	Diving hyperbaric
5	34 F	R, III	32	vascularized bone graft	Alcoholism
6	23 M	R, III	15	vascularized bone graft	corticosteroid, renal disease
7	27 F	R, II	8	vascularized bone graft	Corticosteroid
8	70 F	L, III	2	conservative	Corticosteroid
9	38 F	R, III	4	conservative	Nil
10	46 M	L, II	14	conservative	Nil
11	40 M	R, III	3	conservative	Nil
12	47 M	R, II	150	pediculated bone graft	Diving hyperbaric
13	58 M	R, II	2	conservative	Nil
14	42 M	R, IV	24	total hip replacement	Alcoholism
15	32 M	R, III	27	vascularized bone graft	Nil

*AVN: avascular necrosis

**Duration: interval from unilateral femoral head AVN diagnosis until the contralateral femoral head MRS was performed.

R = right

L = left

Figure 1

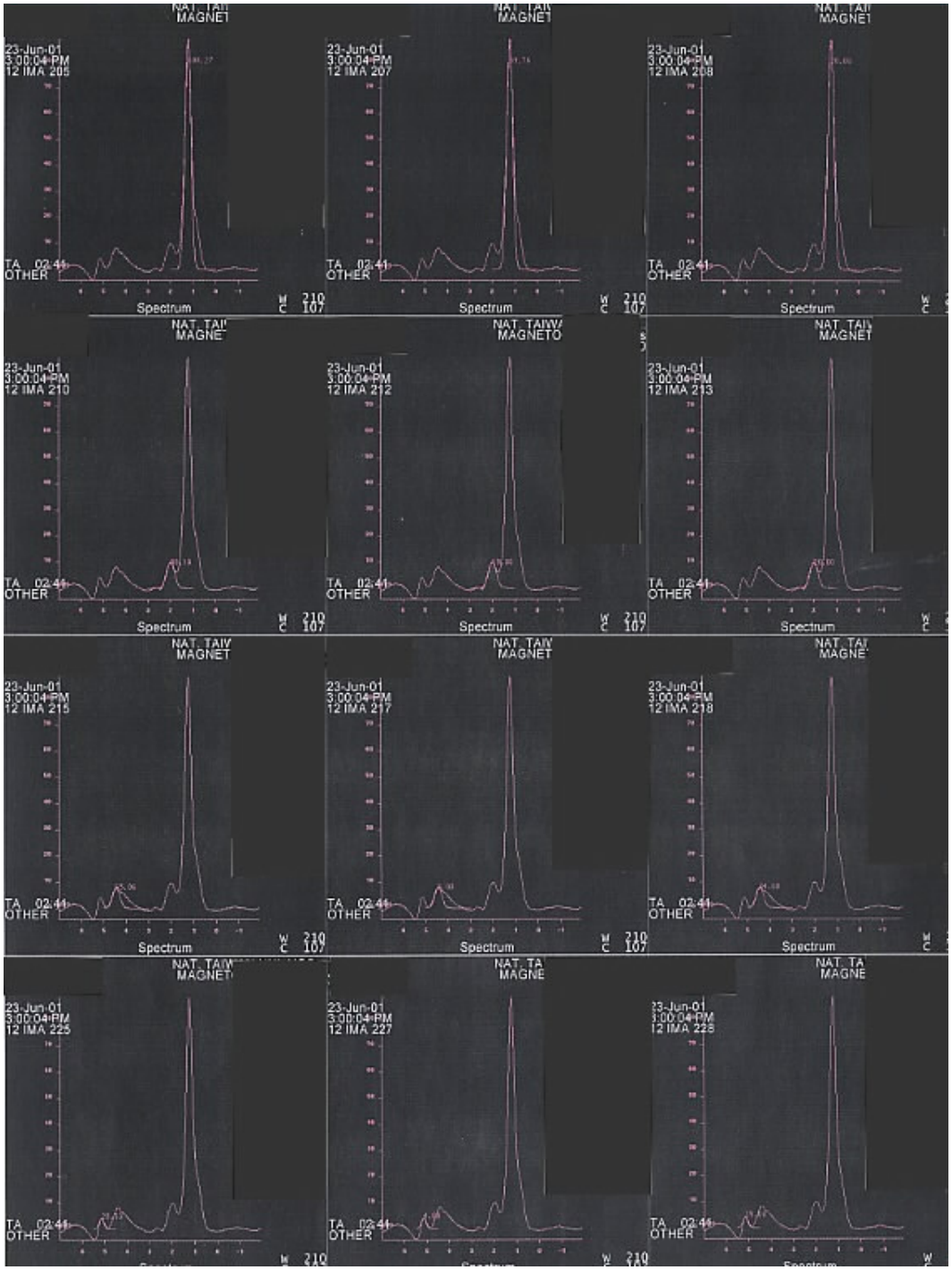
23-Jun-01
3:00:04 PM
12 IMA 205
23-Jun-01
3:00:04 PM
12 IMA 207
23-Jun-01
3:00:04 PM
12 IMA 208
23-Jun-01
3:00:04 PM
12 IMA 210
23-Jun-01
3:00:04 PM
12 IMA 212
23-Jun-01
3:00:04 PM
12 IMA 213
23-Jun-01
3:00:04 PM
12 IMA 215
23-Jun-01
3:00:04 PM
12 IMA 217
23-Jun-01
3:00:04 PM
12 IMA 218
23-Jun-01
3:00:04 PM
12 IMA 225
23-Jun-01
3:00:04 PM
12 IMA 227
TA 02:41
OTHER
Spectrum

Figure 2

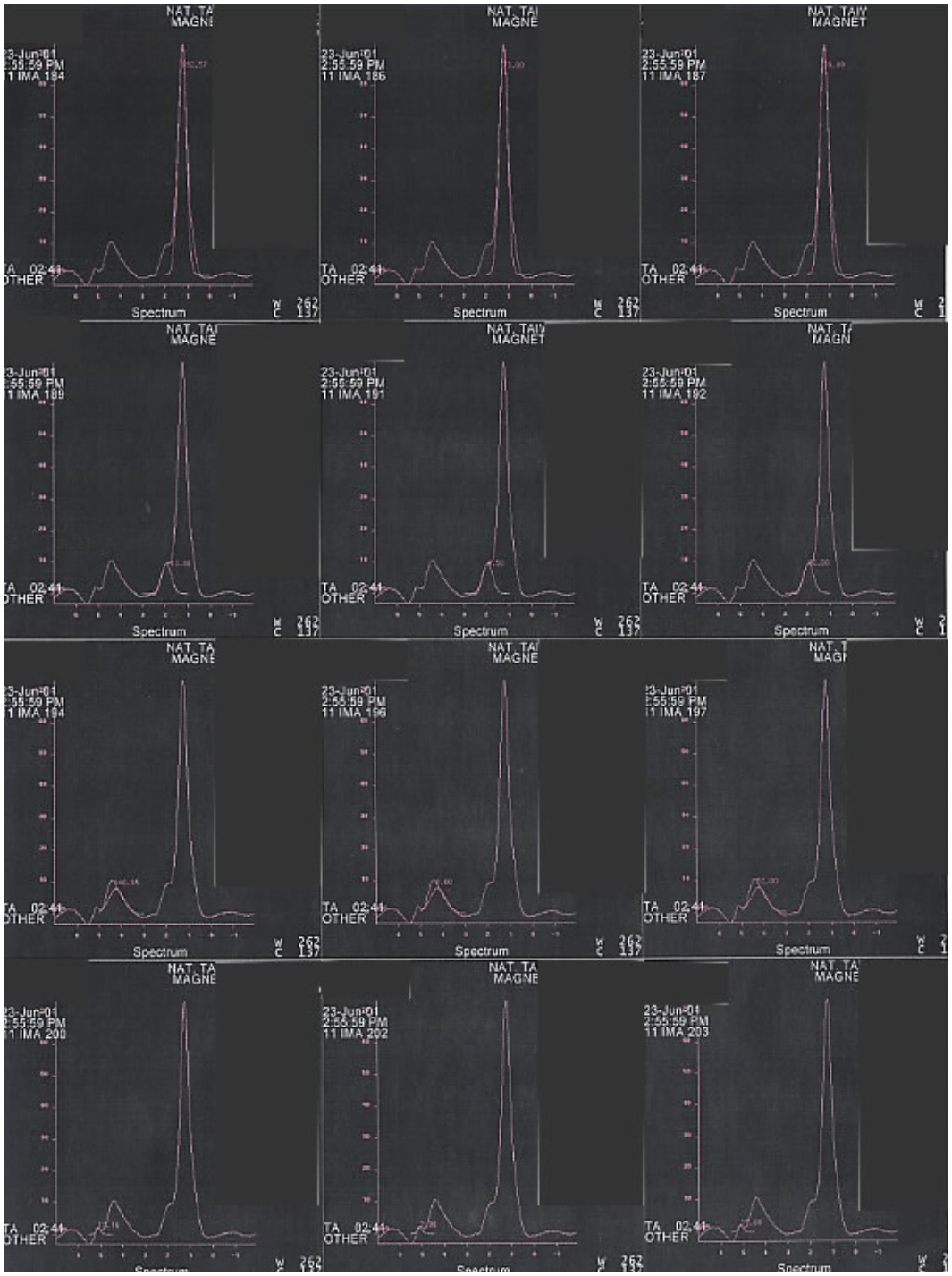
NAT_TA
MAGNE
23-Jun-01
2:55:59 PM
11 IMA_184
TA 02:41
OTHER
Spectrum
W 262
C 137
NAT_TA
MAGNE
23-Jun-01
2:55:59 PM
11 IMA_186
TA 02:41
OTHER
Spectrum
W 262
C 137
NAT_TA
MAGNET
23-Jun-01
2:55:59 PM
11 IMA_187
TA 02:41
OTHER
Spectrum
NAT_TA
MAGNE
23-Jun-01
2:55:59 PM
11 IMA_189
TA 02:41
OTHER
Spectrum
W 262
C 137
NAT_TA
MAGNET
23-Jun-01
2:55:59 PM
11 IMA_191
TA 02:41
OTHER
Spectrum
W 262
C 137
NAT_T
MAGN
23-Jun-01
2:55:59 PM
11 IMA_192
TA 02:41
OTHER
Spectrum
NAT_TA
MAGNE
23-Jun-01
2:55:59 PM
11 IMA_194
TA 02:41
OTHER
Spectrum
W 262
C 137
NAT_TA
MAGNE
23-Jun-01
2:55:59 PM
11 IMA_196
TA 02:41
OTHER
Spectrum
W 262
C 137
NAT_T
MAGI
23-Jun-01
2:55:59 PM
11 IMA_197
TA 02:41
OTHER
Spectrum
NAT_TA
MAGNE
23-Jun-01
2:55:59 PM
11 IMA_200
TA 02:41
OTHER
W 262
NAT_TA
MAGNE
23-Jun-01
2:55:59 PM
11 IMA_202
TA 02:41
OTHER
W 262
NAT_TA
MAGNE
23-Jun-01
2:55:59 PM
11 IMA_203
TA 02:41
OTHER